

D^* and D_s^* distribution amplitudes from Bethe-Salpeter wave functionsFernando E. Serna^{1,2}, Roberto Correa da Silveira,¹ and Bruno El-Bennich¹¹*LFTC, Universidade Cidade de São Paulo, Rua Galvão Bueno 868, São Paulo SP 01506-000, Brazil*²*Departamento de Física, Universidad de Sucre, Carrera 28 No. 5-267, Barrio Puerta Roja, Sincelejo 700001, Colombia*

(Received 15 September 2022; accepted 18 October 2022; published 28 November 2022)

We report on the first calculation of the longitudinal and transverse light front distribution amplitudes of the D^* and D_s^* mesons and their first four moments. As a by-product, we also obtain these distribution amplitudes for the ρ , ϕ , K^* , and J/Ψ mesons and confirm a prediction of lattice QCD for the vector kaon: while the longitudinal distribution amplitude is almost symmetric, the transverse one is oblique implying that the strange quark carries more momentum.

DOI: [10.1103/PhysRevD.106.L091504](https://doi.org/10.1103/PhysRevD.106.L091504)**I. MOTIVATION**

In relativistic quantum field theory the infinite degrees of freedom do not allow for a straightforward definition of a particle's wave function as in quantum mechanics. In particular, in quantum chromodynamics (QCD) the fundamental quark and gluon fields are not even observable. On the other hand, the bound states of antiquark-quark pairs can be described by a Bethe-Salpeter wave function, the closest relative to a wave function in quantum mechanics. Still, in the instant-form of QCD dynamics these wave functions are defined in an infinite-body field theory in which particles interact and their number is not conserved.

One could overcome this difficulty if the hadron's light-front wave function was known exactly, though realistic calculations of hadronic bound states in the front form are a challenging task [1]. A different path to a sensible definition of a wave function in quantum field theory is drawn by projecting the Bethe-Salpeter wave function in the instant form on the light front. Depending on the projection chosen this yields the hadron's light-front wave function or its light-front distribution amplitude (LFDA). The latter describes the longitudinal momentum distribution of valence quarks in the limit of negligible transverse momentum. While they are nonmeasurable objects, they are widely being applied in hadron and flavor physics.

For instance, the asymptotic LFDA of the pion, $\phi(x, \mu) \xrightarrow{\mu \rightarrow \infty} 6x(1-x)$, enters in the expression of its elastic electromagnetic form factor at very large momentum transfers [2,3]. Since the LFDAs are scale-dependent and

become broader at smaller momenta, they directly influence the momentum dependence of the elastic form factors in momentum regions accessible in collider experiments [4–6]. Weak B decays into two light(er) mesons are frequently treated as hard exclusive processes in which the decay amplitude is factorized into perturbative short-distance contributions and a nonperturbative transition amplitude. Here, too, the LFDAs enter both the hard-scattering integrals and the heavy-to-light transition amplitudes [7–11]. More recently, the exclusive electroweak production of $D_s^{(*)}$ mesons on an unpolarized nucleon was investigated in the framework of collinear QCD factorization which also involves the heavy meson's LFDA [12–15].

Beyond its numerous applications in hard exclusive processes, these one-dimensional distributions provide a practical probability interpretation of partons, as in this frame the particle number is conserved. Namely, the distributions $\phi(x, \mu)$ express the light-front fraction of the hadron's momentum that a valence quark carries. Another compelling feature is that one can observe the qualitative and quantitative impact of dynamical chiral symmetry breaking (DCSB) on the LFDA at a given scale μ . For instance, the distribution amplitude $\phi_\pi(x, \mu)$ of the pion is a concave function which clearly evolves from its asymptotic $\mu \rightarrow \infty$ form to a much broader distribution [16]. Similarly, the kaon's distribution amplitude, $\phi_K(x, \mu)$, is not symmetric about the midpoint $x = 1/2$, which expresses nothing but SU(3) flavor symmetry breaking, and that asymmetry is exacerbated with increasing mass difference of the quarks [17,18].

The question arises of how DCSB impacts antiquark-quark states in other J^{PC} channels and an extension to the vector mesons is natural. Moreover, the LFDA of vector mesons arises in the collinear factorization of weak B -decay amplitudes [19] and in diffractive vector-meson production [20,21]. Within the combined framework of the Dyson-Schwinger equation (DSE) and the Bethe-Salpeter equation (BSE) [22]

Published by the American Physical Society under the terms of the Creative Commons Attribution 4.0 International license. Further distribution of this work must maintain attribution to the author(s) and the published article's title, journal citation, and DOI. Funded by SCOAP³.

the LFDAs of the ρ and ϕ mesons were calculated in Ref. [23] and later the LFDAs of heavy quarkonia were obtained in Ref. [24]. In here, using a kindred DSE and BSE framework, we extend earlier work on D and D_s distribution amplitudes [18] to those of their vector partners and make predictions for the twist-2 LFDA of the D^* and D_s^* mesons considering the two-quark Fock-state of their light front wave function. Along the way, we compute the LFDA of the ρ , K^* , ϕ , and J/Ψ mesons and compare them with the distribution amplitudes of other approaches [20,21,24–27].

II. TWIST-TWO DISTRIBUTION AMPLITUDES

A vector meson with total momentum P and mass m_V , $P^2 = -m_V^2$, made of a quark and an antiquark of flavors f and g is described by four twist-two distribution amplitudes, though only two of them are independent at leading twist as a consequence of a Wandzura-Wilczek type of relation [25]. The two LFDAs we consider, $\phi_V^\parallel(x; \mu)$ and $\phi_V^\perp(x; \mu)$, describe the fraction of total momentum on the light front, $x = k^+/P^+ = (k_0 + k_z)/(P_0 + P_z)$, carried by the quark in longitudinally and transversely polarized mesons, respectively. They can be extracted from the Bethe-Salpeter wave function, $\chi_{V\nu}^{fg}(k; P)$, with the following projections onto the light front [23,24]:

$$f_V \phi_V^\parallel(x; \mu) = \frac{m_V N_c \mathcal{Z}_2}{\sqrt{2n \cdot P}} \text{Tr}_D \int^\Lambda \frac{d^4 k}{(2\pi)^4} \delta(n \cdot k_\eta - xn \cdot P) \times \gamma \cdot n n_\nu \chi_{V\nu}^{fg}(k, P), \quad (1)$$

$$f_V^\perp \phi_V^\perp(x; \mu) = -\frac{N_c \mathcal{Z}_T}{2\sqrt{2}} \text{Tr}_D \int^\Lambda \frac{d^4 k}{(2\pi)^4} \delta(n \cdot k_\eta - xn \cdot P) \times n_\mu \sigma_{\mu\rho} \mathcal{O}_{\rho\nu}^\perp \chi_{V\nu}^{fg}(k, P), \quad (2)$$

where $N_c = 3$, $n = (0, 0, 1, i)$ is a lightlike vector and $\bar{n} = \frac{1}{2}(0, 0, -1, i)$ its conjugate with $n^2 = \bar{n}^2 = 0$, $n \cdot P = -m_V$, $\bar{n} \cdot P = -m_V/2$, and $n \cdot \bar{n} = -1$, where we use the Euclidean metric. In Eq. (2) the Dirac commutator $\sigma_{\mu\nu}$ is contracted with the tensor [28],

$$\mathcal{O}_{\rho\nu}^\perp = \delta_{\rho\nu} + n_\rho \bar{n}_\nu + \bar{n}_\rho n_\nu. \quad (3)$$

In Eqs. (1) and (2), $\chi_{V\nu}^{fg}(k; P) = S_f(k_\eta) \Gamma_{V\nu}^{fg}(k, P) S_g(k_{\bar{\eta}})$ is the projected wave function, where $\Gamma_{V\nu}^{fg}(k; P)$ denotes the Bethe-Salpeter amplitude (BSA) and $S_f(k_\eta)$ and $S_g(k_{\bar{\eta}})$ are respectively the quark and antiquark propagators with momenta $k_\eta = k + \eta P$ and $k_{\bar{\eta}} = k - \bar{\eta} P$. The details of their calculation, solving numerically the DSE for the quarks of a given flavor and the BSE for a vector meson, in particular the D and D^* mesons, are provided elsewhere [18,29,30]. The parameters $\eta + \bar{\eta} = 1$ define momentum fractions and Λ is an ultraviolet regularization mass-scale; no observables can depend on η , $\bar{\eta}$, and Λ owing to Poincaré covariance. Furthermore, $\mathcal{Z}_2(\mu, \Lambda)$ is the wave-function

renormalization constant and $\mathcal{Z}_T(\mu, \Lambda)$ is the tensor-vertex renormalization constant of the quark. Both constants as well as f_V^\perp depend on the renormalization scale μ , whereas f_V is renormalization-point independent and measures the strength of the $\rho^0 \rightarrow e^+ e^-$ decay amplitude.

The expressions for $\phi_V^\parallel(x; \mu)$ and $\phi_V^\perp(x; \mu)$ in Eqs. (1) and (2) are not amenable to straightforward numerical integration. Instead, one computes Mellin moments [16],

$$\langle x^m \rangle_{\parallel, \perp} = \int_0^1 x^m \phi_V^{\parallel, \perp}(x, \mu) dx, \quad (4)$$

from which one can reconstruct the distribution amplitudes on the domain $x \in [0, 1]$. The BSA normalization ensures that $\langle x^0 \rangle_{\parallel} = \langle x^0 \rangle_{\perp} = 1$ which in turn defines the vector and tensor decay constants, f_V^\parallel and f_V^\perp .

Integrating both sides of Eqs. (1) and (2) and applying the Dirac-function property $\int_0^1 x^m \delta(a - xb) dx = \frac{a^m}{b^{m+1}} \theta(b - a)$, leads to the expressions,

$$\langle x^m \rangle_{\parallel} = \frac{m_V N_c \mathcal{Z}_2}{\sqrt{2} f_V} \text{Tr}_D \int^\Lambda \frac{d^4 k}{(2\pi)^4} \frac{(n \cdot k_\eta)^m}{(n \cdot P)^{m+2}} \gamma \cdot n n_\nu \chi_{V\nu}^{fg}(k, P), \quad (5)$$

$$\langle x^m \rangle_{\perp} = -\frac{N_c \mathcal{Z}_T}{2\sqrt{2} f_V^\perp} \text{Tr}_D \int^\Lambda \frac{d^4 k}{(2\pi)^4} \frac{(n \cdot k_\eta)^m}{(n \cdot P)^{m+1}} \times n_\mu \sigma_{\mu\rho} \mathcal{O}_{\rho\nu}^\perp \chi_{V\nu}^{fg}(k, P). \quad (6)$$

With this, we are in principle able to compute Mellin moments to arbitrary order m . We do so by employing the numerical solutions of the quark propagators for complex momenta defined by the parabolas, $k_\eta^2 = k^2 - \eta^2 m_V^2 + 2i\eta m_V |k| z_k$ and $k_{\bar{\eta}}^2 = k^2 - \bar{\eta}^2 m_V^2 - 2i\bar{\eta} m_V |k| z_k$, where $z_k = k \cdot P / |k| |P|$, $-1 \leq z \leq +1$, and of the BSA of the vector mesons [30]. That is, other than in Ref. [18], we do not rely on complex-conjugate pole parametrizations of the propagators nor on Nakanishi representations of the BSA, as the latter introduce ambiguities when fitted to numerical solutions. The direct integration comes at the price that we can only access moments up to $m_{\max} = 4-6$, as the numerical error becomes significant for larger moments. These moments, though, are sufficient to reconstruct the desired LFDA.

We proceed as in Refs. [16–18,23,24] and in the case of the light vector mesons we use an expansion in terms of Gegenbauer moments $C_n^\alpha(2x - 1)$, which form a complete orthonormal set on $x \in [0, 1]$ with respect to the measure $[x(1-x)]^{\alpha-1/2}$, in order to reconstruct their two independent twist-two LFDAs ($\bar{x} = 1 - x$):

$$\phi_{V\text{rec}}^{\parallel, \perp}(x, \mu) = \mathcal{N}(\alpha) [x\bar{x}]^{\alpha-\frac{1}{2}} \left[1 + \sum_{n=1}^N a_n C_n^\alpha(2x - 1) \right]. \quad (7)$$

This expansion is employed for neutral mesons as well as for flavored mesons, which are not C -parity eigenstates.

TABLE I. The first four Mellin moments, $\langle x^m \rangle_{\parallel}$ and $\langle x^m \rangle_{\perp}$, of the light vector mesons and the coefficients of their reconstructed Gegenbauer expansion (7). The errors on a_1 , a_2 and α stem from the minimization.

	$\langle x \rangle_{\parallel,\perp}$	$\langle x^2 \rangle_{\parallel,\perp}$	$\langle x^3 \rangle_{\parallel,\perp}$	$\langle x^4 \rangle_{\parallel,\perp}$	$a_1^{\parallel,\perp}$	$a_2^{\parallel,\perp}$	$\alpha^{\parallel,\perp}$
ρ_{\parallel}	0.500	0.312	0.226	0.161	0.0	0.003 ± 0.038	0.908 ± 0.023
ρ_{\perp}	0.500	0.312	0.218	0.160	0.0	-0.136 ± 0.007	0.799 ± 0.006
ϕ_{\parallel}	0.500	0.296	0.195	0.134	0.0	-0.372 ± 0.010	0.864 ± 0.010
ϕ_{\perp}	0.500	0.296	0.193	0.134	0.0	-0.386 ± 0.002	0.870 ± 0.002
K_{\parallel}^*	0.509	0.323	0.236	0.179	0.041 ± 0.027	-0.191 ± 0.048	0.643 ± 0.031
K_{\perp}^*	0.528	0.351	0.262	0.204	0.119 ± 0.003	0.122 ± 0.015	0.840 ± 0.019

In case of the former, the odd components a_n vanish. In fitting the calculated moments in Eqs. (5) and (6), we consider, besides the coefficients a_n , the power α itself a parameter rather than projecting on the $\alpha = 3/2$ basis. This allows to limit the expansion to $N = 2$ and considerably simplifies the fits discussed below [16]. The heavy vector mesons, i.e., the D^* , D_S^* , and J/ψ , are parametrized with a different expression:

$$\phi_{V\text{rec}}^{\parallel,\perp}(x, \mu) = \mathcal{N}(\alpha, \beta) 4x\bar{x} e^{4\alpha x\bar{x} + \beta(x-\bar{x})}. \quad (8)$$

This functional form is more appropriate for a distribution amplitude with a convex-concave-convex functional behavior that tends to a δ -function in the infinite heavy quark limit, as the use of an expansion, such as in Eq. (7), leaves one no choice but to retain a large number of Gegenbauer moments. A very similar functional expression is also found when the Nakanishi weight function is extracted from the quarkonia's Bethe-Salpeter wave function [31]. The normalizations $\mathcal{N}(\alpha)$ and $\mathcal{N}(\alpha, \beta)$ in Eqs. (7) and (8) can be found in Ref. [32].

We thus reconstruct the vector LFDAs by minimizing the sum,

$$\epsilon_{\parallel,\perp} = \sum_{m=1}^{m_{\max}} \left| \frac{\langle x^m \rangle_{\parallel,\perp}^{\text{rec}}}{\langle x^m \rangle_{\parallel,\perp}} - 1 \right|, \quad (9)$$

where the moments $\langle x^m \rangle_{\parallel,\perp}^{\text{rec}}$ are calculated using Eq. (4) and the expansion in either Eq. (7) or Eq. (8), whereas $\langle x^m \rangle_{\parallel,\perp}$ denotes the moments in Eqs. (5) and (6). It is useful to contrast our predictions for the longitudinal and transverse LFDAs with those obtained using other approaches, namely with lattice QCD (LQCD) [26,27], QCD sum rules (QCDSR) [25] and with earlier calculations in the DSE-BSE framework (DSE) [23]. In order to do so we also compute the moments,

$$\langle \xi^{2m} \rangle_{\parallel,\perp} = \int_0^1 \xi^{2m} \phi_{V\text{rec}}^{\parallel,\perp}(x, \mu) dx, \quad (10)$$

in terms of the difference of momentum fractions, $\xi = x - (1-x) = 2x - 1$.

III. RESULTS

We begin with the light vector mesons and determine the coefficients $a_n^{\parallel,\perp}$ of their Gegenbauer expansion via a least-square fit of $\epsilon_{\parallel,\perp}$ (9) with the four moments $\langle x \rangle, \langle x^2 \rangle, \langle x^3 \rangle, \langle x^4 \rangle$. We report their values and those of the corresponding $a_n^{\parallel,\perp}$ of the ρ , ϕ and K^* mesons in Table I and compare the moments $\langle \xi^{2m} \rangle_{\parallel,\perp}$ (10) with other results in Table II.

The LFDAs for the ρ and ϕ mesons are compared in Fig. 1 with the prediction of a DSE-based calculation and the LDFA reconstructed with moments from LQCD, respectively. We infer that the distributions follow the expected pattern: both LFDAs are symmetric about the midpoint, $x = 1/2$. However, the $\phi_{\rho}^{\parallel,\perp}(x, \mu)$ distributions are broad while $\phi_{\phi}^{\parallel,\perp}(x, \mu)$ tend to the asymptotic form

TABLE II. Comparison of $\langle \xi^{2m} \rangle_{\parallel,\perp}$ moments for the ρ , ϕ and K^* mesons. The QCDSR values are obtained with Eq. (4) employing the Gegenbauer expansion (7) with $\alpha = 3/2$ and the value for a_2 in Ref. [25]. Similarly, we fit the tabulated values of $\phi_V^{\parallel}(x; \mu)$ and $\phi_V^{\perp}(x; \mu)$ provided in Ref. [27] with the same Gegenbauer expansion and use them to calculate the moments.

$\rho_{\parallel,\perp}$	$\langle \xi^2 \rangle_{\parallel}$	$\langle \xi^2 \rangle_{\perp}$	$\langle \xi^4 \rangle_{\parallel}$	$\langle \xi^4 \rangle_{\perp}$	$\langle \xi^6 \rangle_{\parallel}$	$\langle \xi^6 \rangle_{\perp}$	$\langle \xi^8 \rangle_{\parallel}$	$\langle \xi^8 \rangle_{\perp}$
Herein	0.263	0.250	0.136	0.127	0.090	0.081	0.062	0.044
DSE [23]	0.231	0.252	0.109	0.126	0.065	0.079	0.044	0.056
QCDSR [25]	0.234	0.238	0.109	0.111	0.063	0.065	0.042	0.043
HERA [20,21]	0.227	0.260	0.105	0.130	0.062	0.079	0.041	0.054
LQCD [26]	0.240(40)							

$\phi_{\parallel,\perp}$	$\langle \xi^2 \rangle_{\parallel}$	$\langle \xi^2 \rangle_{\perp}$	$\langle \xi^4 \rangle_{\parallel}$	$\langle \xi^4 \rangle_{\perp}$	$\langle \xi^6 \rangle_{\parallel}$	$\langle \xi^6 \rangle_{\perp}$	$\langle \xi^8 \rangle_{\parallel}$	$\langle \xi^8 \rangle_{\perp}$
Herein	0.186	0.182	0.077	0.073	0.042	0.039	0.026	0.024
DSE [23]	0.233	0.253	0.111	0.127	0.067	0.080	0.046	0.056
QCDSR [25]	0.245	0.238	0.115	0.111	0.068	0.065	0.045	0.043
LQCD [27]	0.212	0.250	0.097	0.127	0.057	0.081	0.039	0.058

$K_{\parallel,\perp}^*$	$\langle \xi^2 \rangle_{\parallel}$	$\langle \xi^2 \rangle_{\perp}$	$\langle \xi^4 \rangle_{\parallel}$	$\langle \xi^4 \rangle_{\perp}$	$\langle \xi^6 \rangle_{\parallel}$	$\langle \xi^6 \rangle_{\perp}$	$\langle \xi^8 \rangle_{\parallel}$	$\langle \xi^8 \rangle_{\perp}$
Herein	0.272	0.298	0.146	0.164	0.097	0.109	0.072	0.080
QCDSR [25]	0.227	0.227	0.104	0.104	0.060	0.060	0.039	0.039
LQCD [27]	0.200	0.292	0.088	0.162	0.050	0.111	0.032	0.084

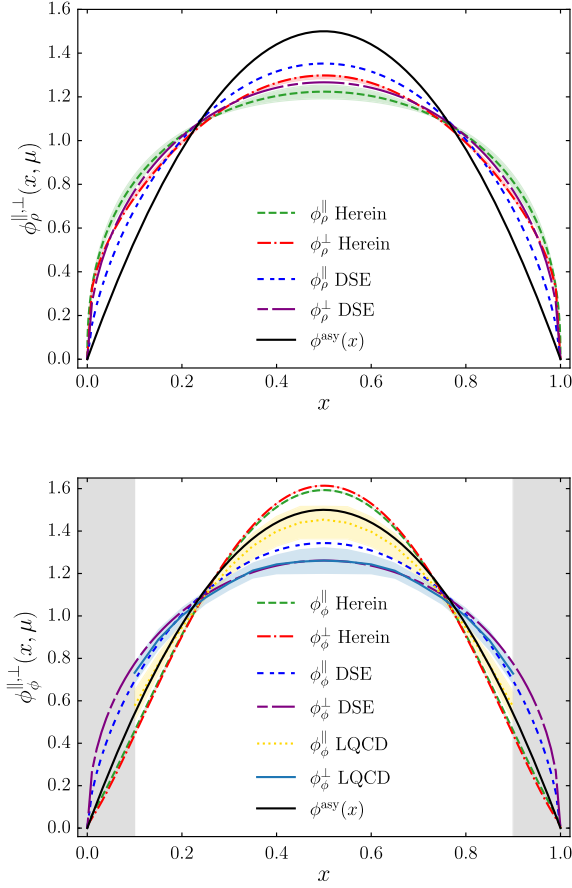


FIG. 1. Comparison of the LFDAs for the ρ (top panel) and ϕ (bottom panel) mesons with those of Refs. [23] (DSE) and [27] (LQCD) at $\mu = 2$ GeV. Error bands reflect the uncertainties of the fit parameters. The intervals $0 \leq x < 0.1$, $1 \geq x > 0.9$ are shaded, as LQCD does not provide data for these momentum fractions due to systematic errors. For comparison, we plot the asymptotic LFDA $\phi(x, \mu) \xrightarrow{\mu \rightarrow \infty} 6x\bar{x}$.

$\phi(x) \xrightarrow{\mu \rightarrow \infty} 6x\bar{x}$. In addition, we observe that $\phi_\rho^{\parallel}(x, \mu)$ is slightly broader than $\phi_\rho^{\perp}(x, \mu)$, the origin of which are the different values of a_2^{\parallel} and a_2^{\perp} in Table I. It appears from Table II that our calculated $\langle \xi^{2m} \rangle_{\parallel}$ moments for the ρ meson are overall about 11% larger, whereas the values for $\langle \xi^{2m} \rangle_{\perp}$ are in very good agreement with those of Ref. [23] and the HERA fit [20,21].

In the case of the ϕ -meson, we note that $\phi_\phi^{\parallel}(x, \mu) \approx \phi_\phi^{\perp}(x, \mu)$ since $a_2^{\parallel} \approx a_2^{\perp}$ and $\alpha^{\parallel} \approx \alpha^{\perp}$. We remark that our results for $\phi_\phi^{\parallel, \perp}(x, \mu)$ differ from those in Ref. [23] as can be inferred from Fig. 1. The reason for this, despite a like-minded BSE approach, is that we use a larger strange-quark mass, $m_s = 166$ MeV at $\mu = 2$ GeV. With a lower value of $m_s \approx 100$ MeV we find similar distributions as in Ref. [23]. However, we prefer to renormalize the DSE with a larger strange mass as it results in a more consistent description of the K , K^* , D_s^* and ϕ mesons.

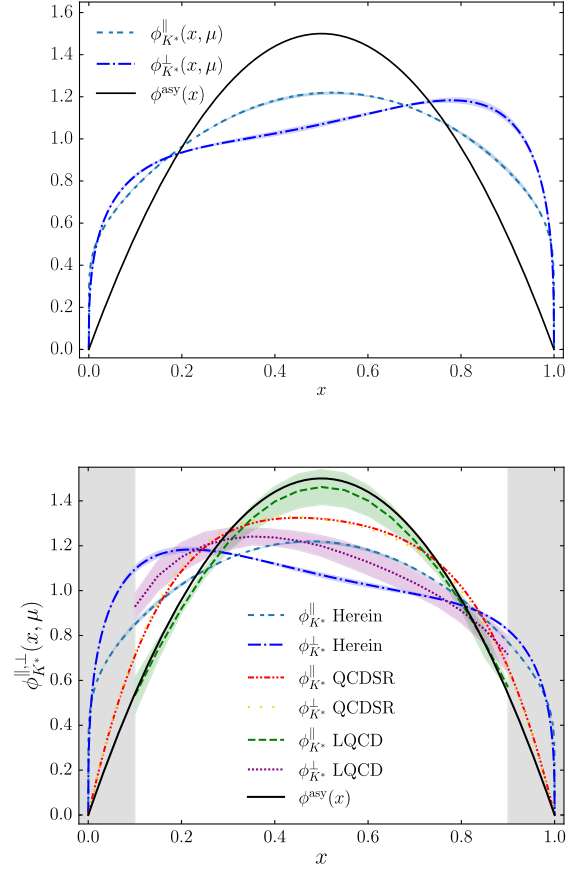


FIG. 2. Top panel: longitudinal and transverse distribution amplitudes, $\phi_{K^*}^{\parallel}(x, \mu)$ and $\phi_{K^*}^{\perp}(x, \mu)$ for $\mu = 2$ GeV. Bottom panel: Comparison of our predictions for the K^* with those of QCDSR [25] and LQCD [27], where we replaced $x \rightarrow 1 - x$ in Eq. (9). The shaded areas and error bands are as in Fig. 1.

We now turn our attention to the K^* and present the longitudinal and transverse LFDAs in Fig. 2, where we juxtapose them with predictions from LQCD and QCDSR. Notably, the longitudinal distribution is a concave, nearly symmetric function of x , much broader than the asymptotic form, which is a consequence of the smallness of the a_1^{\parallel} coefficient. The transverse LFDA, on the other hand, is asymmetric around the midpoint and its maximum is located at $x = 0.78$, which clearly indicates SU(3) flavor symmetry breaking. The asymmetric shape is due to the similarity of the Gegenbauer coefficients, $a_1^{\perp} \approx a_2^{\perp}$ whereas $a_1^{\parallel} \ll a_2^{\parallel}$, see Table I. This is in agreement with a recent calculation in LQCD, though in that study $\phi_{K^*}^{\parallel}(x, \mu)$ tends toward the asymptotic distribution [27]. In contrast to these findings, QCDSR predicts $\phi_{K^*}^{\parallel}(x, \mu) \approx \phi_{K^*}^{\perp}(x, \mu)$ [25].

As we noted earlier, the heavier vector charmonium and charmed mesons require a modified description of their LFDA (8) to fit the moments. We report these moments, $\langle x^m \rangle_{\parallel}$ and $\langle x^m \rangle_{\perp}$, for the J/Ψ , D^* and D_s^* in Table III. The distributions $\phi_{J/\Psi}^{\parallel}(x, \mu)$ and $\phi_{J/\Psi}^{\perp}(x, \mu)$ we then reconstruct

TABLE III. Mellin moments $\langle x^m \rangle_{\parallel}$ and $\langle x^m \rangle_{\perp}$ of the J/Ψ , D^* and D_s^* mesons. Fitting these moments with their definition in Eq. (4) and the corresponding $\phi_{V^{\parallel,\perp}}^{\parallel,\perp}(x, \mu)$ parametrization (8) yields $\alpha_{\parallel,\perp}$ and $\beta_{\parallel,\perp}$ and accompanying fit errors.

	$\langle x \rangle_{\parallel,\perp}$	$\langle x^2 \rangle_{\parallel,\perp}$	$\langle x^3 \rangle_{\parallel,\perp}$	$\langle x^4 \rangle_{\parallel,\perp}$	$\alpha_{\parallel,\perp}$	$\beta_{\parallel,\perp}$
J/Ψ_{\parallel}	0.500	0.274	0.159	0.097	4.549 ± 0.411	0.081 ± 0.051
J/Ψ_{\perp}	0.500	0.259	0.139	0.076	12.703 ± 1.931	0.004 ± 0.710
D_{\parallel}^*	0.694	0.511	0.396	0.315	0.531 ± 0.207	2.460 ± 0.131
D_{\perp}^*	0.742	0.589	0.471	0.389	0.094 ± 0.001	3.073 ± 0.001
$D_{s\parallel}^*$	0.627	0.418	0.294	0.217	2.582 ± 0.651	2.263 ± 0.296
$D_{s\perp}^*$	0.655	0.465	0.346	0.272	0.448 ± 0.305	1.832 ± 0.136

are plotted in Fig. 3. They are reminiscent of their pseudo-scalar counterpart, i.e., the LFDA of the η_c , which exhibits the same *convex-concave-convex* functional behavior and is more sharply peaked than the asymptotic LFDA [18]. It turns out that the longitudinal distribution is broader and less localized as a function of x than the transverse distribution, an observation also made in Ref. [24].

We conclude this section with a first prediction of the D^* and D_s^* meson distribution amplitudes which we compute with the projections in Eqs. (1) and (2) of the Bethe-Salpeter wave functions. The latter are taken from Ref. [30]; see Table 4 therein for the corresponding masses and weak decay constants. The distributions we reconstruct from $\langle x^m \rangle_{\parallel}$ and $\langle x^m \rangle_{\perp}$ listed in Table III are shown in Fig. 4. Clearly, in both cases the LFDAs are asymmetric and $\phi_{D^*}^{\parallel}(x, \mu)$ and $\phi_{D^*}^{\perp}(x, \mu)$ peak at about $x \approx 0.8-0.85$, while $\phi_{D_s^*}^{\parallel}(x, \mu)$ and $\phi_{D_s^*}^{\perp}(x, \mu)$ reach their maximum in the range $x \approx 0.65-0.8$.

This is readily interpreted as the charm quark carrying most of the light-front momentum in the D^* meson, but less so in the D_s^* meson. Interestingly, the transverse distributions are more asymmetric and the charm seems to carry a larger fraction of the meson momentum than in the longitudinal distribution. Arguably, this observation generalizes our results for the K^* , where the much smaller mass difference between the strange and up quarks leads to an

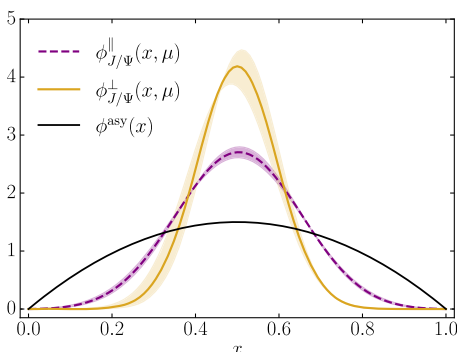


FIG. 3. Longitudinal and transverse J/Ψ distributions. The error bands reflect the uncertainties in $\alpha_{\parallel,\perp}$ and $\beta_{\parallel,\perp}$.

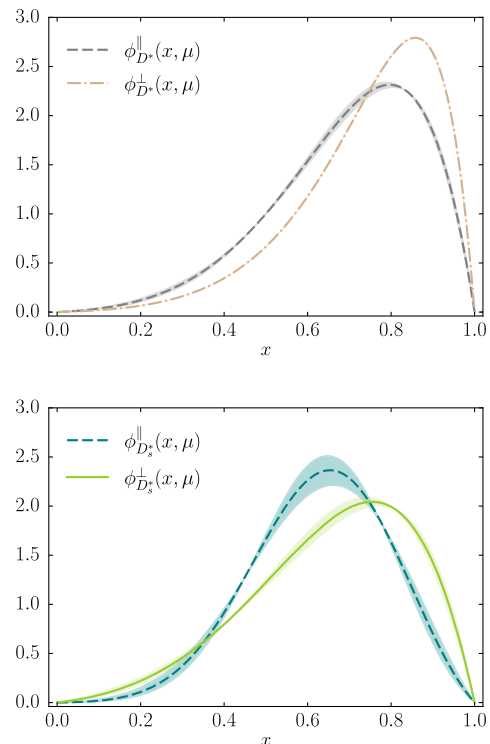


FIG. 4. Longitudinal and transverse LFDAs of the D^* and D_s^* mesons at $\mu = 2$ GeV; error bands as in Fig. 3.

almost symmetric form of $\phi_{K^*}^{\parallel}(x, \mu)$ and to a broad yet asymmetric function $\phi_{K^*}^{\perp}(x, \mu)$.

IV. CONCLUSION

We extracted the LFDAs of the ρ , ϕ , K^* , J/Ψ , D^* , and D_s^* mesons from their Bethe-Salpeter wave functions, which we calculated in Refs. [29,30], with two projections onto the light front given by Eqs. (1) and (2). The transverse LFDA of the ρ meson is in very good agreement with that obtained in a similar DSE-BSE approach [23] and with the HERA fit [20,21], while our longitudinal moments, $\langle z^m \rangle_{\parallel}$, are generally about 11% larger than those in the literature.

We then presented the first calculation of the $\phi_{K^*}^{\parallel}(x, \mu)$ and $\phi_{K^*}^{\perp}(x, \mu)$ within the DSE-BSE framework and confirm the functional form found with LQCD simulations [27]: while the longitudinal distribution of the K^* is almost symmetric about the midpoint $x = 1/2$, the transverse distribution is broad and slanted, which we interpret as the strange quark carrying the larger fraction of the meson's momentum. In the heavy meson sector, both LFDAs of the J/Ψ are alike with that of the η_c , i.e., they are symmetric and narrow, yet not merely concave distributions.

Last not least, we extended our studies in Ref. [18] to the longitudinal and transverse LFDAs of the D^* and D_s^* mesons, a first calculation of these distributions to our knowledge. Our findings are in line with observations for the pseudoscalar D and D_s mesons [18]: the distributions

are asymmetric and reach their maximum at large momentum fractions, namely $x \approx 0.65-0.85$. In other words, the charm quark is most likely to carry the largest fraction of the $D_{(s)}^*$ -momentum, and this is even more so the case for the transverse distribution.

We remind that we provided all the analytic parametrizations of the LFDAs discussed in this work and the parameters are found in Tables I and III. Therefore, the LFDAs of the J/Ψ and $D_{(s)}^*$ mesons can readily be used in diffractive vector-meson production and are of interest to the experimental program of the Electron-Ion Collider.

ACKNOWLEDGMENTS

We acknowledge helpful discussions with Peter Tandy and Minghui Ding. B. E. and F. E. S. participate in the Brazilian network project *INCT-Física Nuclear e Aplicações*, No. 464898/2014-5. This work was supported by the São Paulo Research Foundation (FAPESP), Grant No. 2018/20218-4, and by the National Council for Scientific and Technological Development (CNPq), Grant No. 428003/2018-4. F. E. S. is a CAPES-PNPD postdoctoral fellow financed by Grant No. 88882.314890/2013-01.

-
- [1] W. de Paula, E. Ydrefors, J. H. Alvarenga Nogueira, T. Frederico, and G. Salmè, *Phys. Rev. D* **103**, 014002 (2021).
- [2] A. V. Efremov and A. V. Radyushkin, *Theor. Math. Phys.* **42**, 97 (1980).
- [3] G. P. Lepage and S. J. Brodsky, *Phys. Rev. D* **22**, 2157 (1980).
- [4] L. Chang, I. C. Cloët, C. D. Roberts, S. M. Schmidt, and P. C. Tandy, *Phys. Rev. Lett.* **111**, 141802 (2013).
- [5] K. Raya, L. Chang, A. Bashir, J. J. Cobos-Martínez, L. X. Gutiérrez-Guerrero, C. D. Roberts, and P. C. Tandy, *Phys. Rev. D* **93**, 074017 (2016).
- [6] K. Raya, A. Bashir, and P. Roig, *Phys. Rev. D* **101**, 074021 (2020).
- [7] M. Beneke and M. Neubert, *Nucl. Phys.* **B651**, 225 (2003).
- [8] C. W. Bauer, D. Pirjol, I. Z. Rothstein, and I. W. Stewart, *Phys. Rev. D* **72**, 098502 (2005).
- [9] B. El-Bennich, A. Furman, R. Kaminski, L. Lesniak, and B. Loiseau, *Phys. Rev. D* **74**, 114009 (2006).
- [10] B. El-Bennich, A. Furman, R. Kaminski, L. Lesniak, B. Loiseau, and B. Moussallam, *Phys. Rev. D* **79**, 094005 (2009); **83**, 039903(E) (2011).
- [11] O. Leitner, J. P. Dedonder, B. Loiseau, and B. El-Bennich, *Phys. Rev. D* **82**, 076006 (2010).
- [12] B. Pire and L. Szymanowski, *Phys. Rev. Lett.* **115**, 092001 (2015).
- [13] B. Pire and L. Szymanowski, *Phys. Rev. D* **96**, 114008 (2017).
- [14] B. Pire, L. Szymanowski, and J. Wagner, *Phys. Rev. D* **95**, 094001 (2017).
- [15] B. Pire, L. Szymanowski, and J. Wagner, *Phys. Rev. D* **104**, 094002 (2021).
- [16] L. Chang, I. C. Cloët, J. J. Cobos-Martínez, C. D. Roberts, S. M. Schmidt, and P. C. Tandy, *Phys. Rev. Lett.* **110**, 132001 (2013).
- [17] C. Shi, C. Chen, L. Chang, C. D. Roberts, S. M. Schmidt, and H. S. Zong, *Phys. Rev. D* **92**, 014035 (2015).
- [18] F. E. Serna, R. C. da Silveira, J. J. Cobos-Martínez, B. El-Bennich, and E. Rojas, *Eur. Phys. J. C* **80**, 955 (2020).
- [19] M. Beneke and T. Feldmann, *Nucl. Phys.* **B592**, 3 (2001).
- [20] J. R. Forshaw and R. Sandapen, *J. High Energy Phys.* **11** (2010) 037.
- [21] J. R. Forshaw and R. Sandapen, *Phys. Rev. Lett.* **109**, 081601 (2012).
- [22] A. Bashir, L. Chang, I. C. Cloët, B. El-Bennich, Y. X. Liu, C. D. Roberts, and P. C. Tandy, *Commun. Theor. Phys.* **58**, 79 (2012).
- [23] F. Gao, L. Chang, Y. X. Liu, C. D. Roberts, and S. M. Schmidt, *Phys. Rev. D* **90**, 014011 (2014).
- [24] M. Ding, F. Gao, L. Chang, Y. X. Liu, and C. D. Roberts, *Phys. Lett. B* **753**, 330 (2016).
- [25] P. Ball, V. M. Braun, and A. Lenz, *J. High Energy Phys.* **08** (2007) 090.
- [26] P. A. Boyle *et al.* (RBC and UKQCD Collaborations), *Proc. Sci. LATTICE2008* (**2008**) 165.
- [27] J. Hua, M.-H. Chu, P. Sun, W. Wang, J. Xu, Y.-B. Yang, J.-H. Zhang, and Q.-A. Zhang (Lattice Parton Collaboration), *Phys. Rev. Lett.* **127**, 062002 (2021).
- [28] Y. Lu, D. Binosi, M. Ding, C. D. Roberts, H. Y. Xing, and C. Xu, *Eur. Phys. J. A* **57**, 115 (2021).
- [29] F. F. Mojica, C. E. Vera, E. Rojas, and B. El-Bennich, *Phys. Rev. D* **96**, 014012 (2017).
- [30] B. El-Bennich and F. E. Serna, *Proc. Sci. CHARM2020* (**2021**) 025.
- [31] F. Gao, L. Chang, and Y. x. Liu, *Phys. Lett. B* **770**, 551 (2017).
- [32] F. E. Serna and B. El-Bennich, *Proc. Sci. CHARM2020* (**2021**) 047.